Shaping the output pulse of a linear-transformer-driver module

W. A. Stygar,[1] W. E. Fowler,[1] K. R. LeChien,[1] F. W. Long,[1] M. G. Mazarakis,[1] G. R. McKee,[1] J. L. McKenney,[1] J. L. Porter,[1] M. E. Savage,[1] B. S. Stoltzfus,[1] D. M. Van De Valde,[2] and J. R. Woodworth[1]

[1]*Sandia National Laboratories, Albuquerque, New Mexico 87185, USA*

[2]*EG&G, Albuquerque, New Mexico 87107, USA*

(Received 23 November 2008; published 10 March 2009)

We demonstrate that a wide variety of current-pulse shapes can be generated using a linear-transformer-driver (LTD) module that drives an internal water-insulated transmission line. The shapes are produced by varying the timing and initial charge voltage of each of the module's cavities. The LTD-driven accelerator architecture outlined in [Phys. Rev. ST Accel. Beams **10**, 030401 (2007)] provides additional pulse-shaping flexibility by allowing the modules that drive the accelerator to be triggered at different times. The module output pulses would be combined and symmetrized by water-insulated radial-transmission-line impedance transformers [Phys. Rev. ST Accel. Beams **11**, 030401 (2008)].

DOI: 10.1103/PhysRevSTAB.12.030402 PACS numbers: 84.70.+p, 84.60.Ve, 52.58.Lq

I. INTRODUCTION

A linear-transformer-driver (LTD) module consists of a number of inductive LTD cavities connected in series to achieve voltage addition [1–37]. Hence, an LTD module is a type of induction voltage adder (IVA) [38]. Unlike a conventional IVA, each cavity of an LTD module is driven by capacitors and switches that are located within the cavity itself; consequently, an LTD module is inherently more compact than an IVA driven by external pulsed-power machines.

IVAs were originally designed to drive a *vacuum* magnetically insulated transmission line (MITL) [38]. For such an IVA, part of the MITL is located within, and is concentric to, the IVA's cavities. Following this precedent, Kovalchuk *et al.* [1,5,12], Mazarakis *et al.* [6,8,11,25,29,31,32,36], Kim *et al.* [15,18,33], Rose *et al.* [17,27], Leckbee *et al.* [22,24,28], Olson [26], and Gomez *et al.* [35] developed designs of LTD modules that drive an internal MITL. Such modules have been considered for z-pinch-physics [1,5,8,11,25,29,31–33,35,36], x-ray-radiography [6,11,15,17,18,22,24,27,28], excimer-laser [12], and inertial-confinement-fusion (ICF) [25,26,29,31] applications.

Kim and colleagues consider instead an LTD module that drives an internal *oil-insulated* transmission line [9]; Corcoran, Smith, and co-workers [10,14] consider the use of an internal *water-insulated* line. Reference [37] is the first to propose that water-insulated LTD modules be used to drive next-generation pulsed-power accelerators. A 1000-TW LTD-driven accelerator [37], such as the one illustrated by Fig. 1, could be used to drive z-pinch loads for high-energy-density and ICF-physics experiments conducted over presently inaccessible parameter regimes.

In this article, we demonstrate that the LTD-driven accelerator outlined in Ref. [37], and illustrated by Fig. 1, could also be used to generate a wide variety of current-pulse shapes. Such a capability is of interest to material-dynamics experiments, which usually require a precisely shaped current pulse [39–43]. Pulse shaping is also of interest to z-pinch experiments, which may demonstrate an increase in the x-ray power and energy radiated by a pinch when the time history of the pinch current is optimized [44–47]. The accelerator outlined by Fig. 1 would allow material-dynamics and z-pinch experiments to be driven by an electrical power as high as 1000 TW, which is an order of magnitude greater than is presently available. We also observe that a *single* water-insulated LTD module could be used to drive a radiographic electron-beam diode, and would be capable of providing a shaped current pulse to optimize diode performance [48,49].

The accelerator illustrated by Fig. 1 is driven by 210 LTD modules, each of which consists of 60 identical LTD cavities connected in series [37]. A cross-sectional view of a single module is presented by Fig. 2. To demonstrate that the accelerator of Fig. 1 could produce a shaped current pulse, we consider in this article a single module. We assume that the module drives a water-insulated transmission line that is concentric to, and is located within, the cavities. We assume that the line is terminated in a load that has the same impedance as that of the transmission line at the output of the module. We limit the discussion in this article to this idealized case to prove the concept; we do not consider the various types of loads that might be used in an experiment, and how the loads might affect the pulse shape.

In Sec. II, we present several pulse shapes that can be produced by a single LTD module. The discussion of Sec. II assumes that the switches of each of the module's cavities are triggered within τ_c seconds of the triggering of the switches in an adjacent cavity, where τ_c is the time it takes an electromagnetic pulse to propagate (down the internal water-insulated transmission line) the length of a

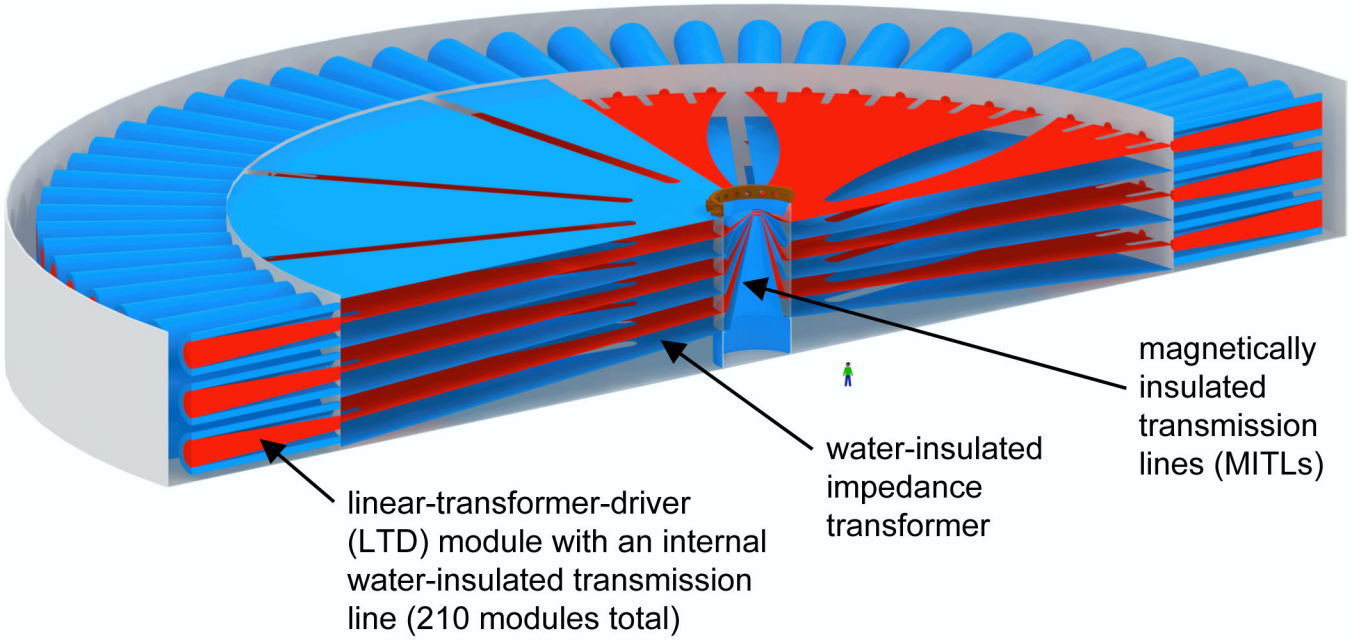

FIG. 1. (Color) Conceptual design of a 1000-TW LTD-driven pulsed-power accelerator [37]. The illustration is approximately to scale. The diameter of the outer-tank wall is 104 m. The illustration includes a person standing near the central MITL section.

single cavity. This guarantees that the switches of each cavity are transit-time isolated from the switches of the other cavities in the module. The isolation prevents the voltage across a given switch, before it is triggered, from being altered by pulses produced by switches in the other cavities. In Sec. III, we explore the results of a slight deviation from the transit-time-isolation constraint. In Sec. IV we present suggestions for future work.

The accelerator architecture represented by Fig. 1 assumes the use of long water-insulated transmission lines to connect the LTD-module drivers to the central region of the accelerator. The use of such lines follows naturally from the use of modules that drive an internal water-insulated line. In Appendix A, we discuss briefly the use of long MITLs instead of long water lines. In Appendices B and C, we estimate the optimum output impedance and minimum current rise time, respectively, of an n-cavity LTD module under a certain set of conditions.

II. PULSE SHAPING WHEN $|t_{j+1} - t_j| \leq \tau_c$

An idealized representation of the first three cavities of an LTD module is given by Fig. 3(a). For this figure, and all

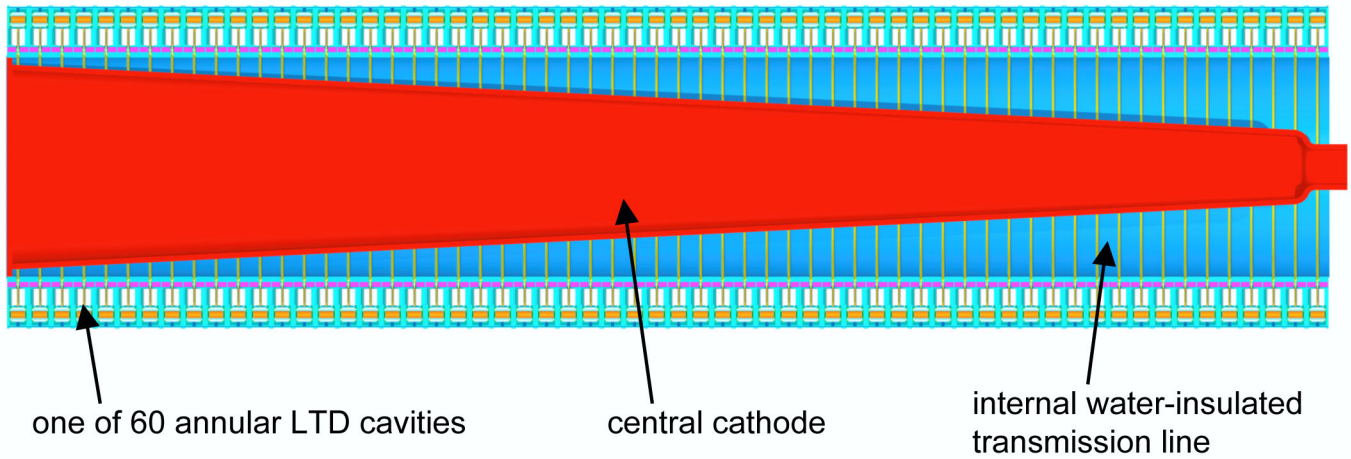

FIG. 2. (Color) Cross-sectional view of a single 60-cavity LTD module. A total of 210 such modules would drive the accelerator illustrated by Fig. 1. The outer diameter of the module is 3 m.

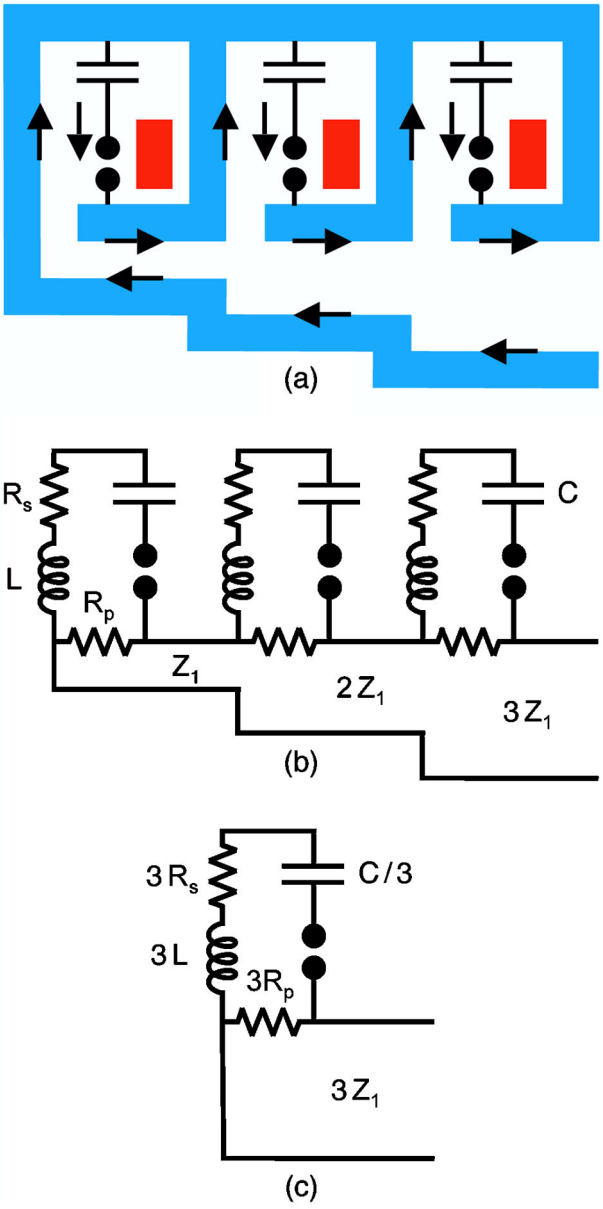

FIG. 3. (Color) (a) Idealized representation of an LTD module with three identical cavities connected in series. A cavity normally contains a number of capacitors and switches; these are represented here by a single capacitor and a single switch. The red rectangles represent inductive high-permeability magnetic cores. The arrows represent the path of *most* of the current flow, after all the switches in the cavities have closed. A small fraction of the current flows around the cores. The LTD module assumed in this article consists of 60 identical cavities. (b) Circuit model of the three-cavity module. (c) Equivalent circuit model of the module. The circuit of (c) is valid only when the switches of each cavity close at a time τ_c later than the closure of the switches in the cavity immediately upstream (i.e., immediately to the left), where τ_c is the time it takes an electromagnetic pulse to propagate (down the internal transmission line) the length of a single cavity. τ_c is the one-way transit time of a single transmission-line segment. We make the simplifying assumption that all the cavities, and all the transmission-line segments, have the same electrical length.

the modules considered in this article, we assume

$$Z_j = jZ_1 = \frac{jZ_n}{n}, \tag{1}$$

$$\tau_{c,j} = \tau_c. \tag{2}$$

The quantity Z_j is the impedance of the transmission-line segment driven by the module's jth cavity; Z_n is the impedance of the transmission line of the final cavity, at the output of the module; $\tau_{c,j}$ is the time it takes an electromagnetic pulse to propagate (down the internal water-insulated transmission line) the length of the jth cavity; and τ_c is a constant.

For definitiveness, we consider the 60-cavity LTD module described in Ref. [37] and illustrated by Fig. 2. Similar results are obtained for modules with different parameters.

We assume each cavity of the 60-cavity module can be modeled as suggested by Fig. 3(b). We also assume the following [9,11,20,25,37]:

$$R_s = 0.015\ \Omega, \tag{3}$$

$$L = 7.5\ \text{nH}, \tag{4}$$

$$C = 800\ \text{nF}, \tag{5}$$

$$R_p = 1.472\ \Omega, \tag{6}$$

$$Z_n = 6.72\ \Omega, \tag{7}$$

$$n = 60, \tag{8}$$

$$\tau_c = 6.6\ \text{ns}. \tag{9}$$

The quantity R_s is that part of the *series* resistance of a single LTD cavity that is due primarily to the switches and capacitors of the cavity. L and C are the inductance and capacitance, respectively, of a single cavity. R_p is the effective *parallel* resistance of a cavity; this circuit element is used to account for energy loss to the cavity's inductive high-permeability magnetic cores [20,21]. Our circuit model assumes that nonlinearities due to the cores can be neglected. Hence, the model is applicable only when the core in each cavity has a sufficient volt-second product to support the cavity's desired voltage time history over the period of interest.

The value for R_p given by Eq. (6) assumes the results presented by Kim and colleagues in Ref. [20], and that 50-μm-thick magnetic tape is used to fabricate the cores [20]. The value for Z_n given by Eq. (7) is estimated as discussed in Appendix B.

Five possible current-pulse shapes that can be produced by the LTD module described above are plotted by Fig. 4. The shapes assume Eqs. (1)–(9), and are calculated by performing SCREAMER [50–52] circuit simulations of the

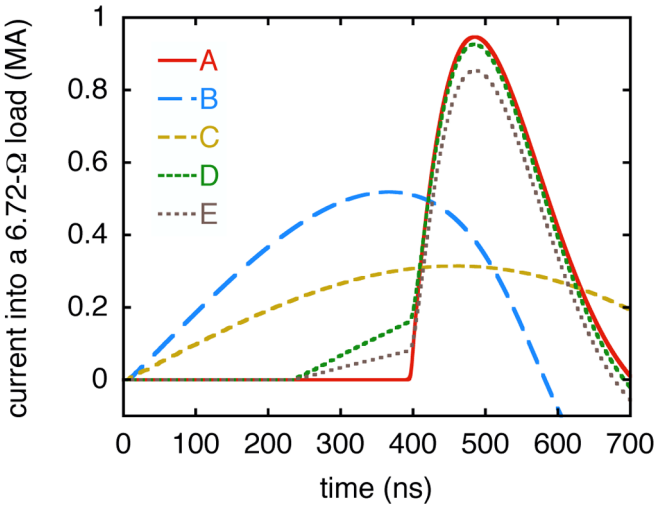

FIG. 4. (Color) Five possible current-pulse shapes that can be produced by a single 60-cavity LTD module driving a matched load. The five shapes are generated by the cavity-triggering sequences plotted by Fig. 5. For current shapes A, B, C, and D, all the cavities are charged to 200 kV. For shape E, cavities 49–60 are charged to 100 kV.

operation of the module. The cavity-triggering sequences used to generate the five shapes are plotted by Fig. 5.

As indicated by Fig. 5, current-pulse-shape A (of Fig. 4) is achieved when the switches of each cavity are closed at a time τ_c later than the closure of the switches in the cavity immediately *upstream* (i.e., the cavity to the left). For this cavity-triggering sequence

$$t_{j+1} - t_j = \tau_c \tag{10}$$

for all values of j between 1 and $n - 1$, where t_j is the time

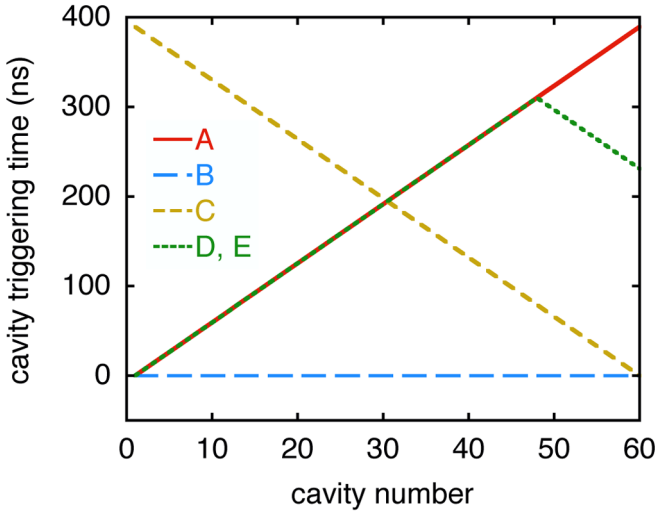

FIG. 5. (Color) Cavity-triggering sequences used to generate the five current-pulse shapes plotted by Fig. 4. For current shapes A, B, C, and D, all the cavities are charged to 200 kV. For shape E, cavities 49–60 are charged to 100 kV.

at which the jth cavity is triggered. Current-shape A assumes each cavity is charged to an initial voltage of 200 kV, which would be accomplished using the +100 kV, −100 kV charging system that was first proposed by Savage [53].

When all the cavities are triggered simultaneously instead of sequentially as described above, the current shape produced is that labeled B. For this triggering sequence

$$t_{j+1} - t_j = 0. \tag{11}$$

Shape C is produced when the switches of each cavity close at a time τ_c later than the closure of the switches in the cavity immediately *downstream* (i.e., the cavity to the right):

$$t_{j+1} - t_j = -\tau_c. \tag{12}$$

As suggested by Fig. 5, current shapes D and E have identical cavity-timing sequences. Shape D is achieved by charging all the cavities to 200 kV, whereas E is achieved by charging cavities 49–60 to 100 kV. (To optimize the performance of an LTD cavity at a lower initial charge voltage would require a lower gas pressure in the cavity's switches.) We note that for sequences D and E, the quantity $t_{j+1} - t_j$ is not the same for all the cavities of the module.

For all five timing sequences plotted by Fig. 5, the switches of each cavity are triggered within τ_c seconds of the triggering of the switches in an adjacent cavity. Hence, all five sequences satisfy the following constraint:

$$|t_{j+1} - t_j| \leq \tau_c \tag{13}$$

for all the cavities. This constraint guarantees that the voltage across each switch is not altered before it is triggered. The constraint would be made less restrictive by increasing τ_c, which could be accomplished by inserting a spacer between every pair of adjacent cavities. As suggested above, the quantity $t_{j+1} - t_j$ need not be the same for all values of j to satisfy the transit-time-isolation requirement; in fact, the quantity $t_{j+1} - t_j$ could be different for each j, as long as Eq. (13) is satisfied.

The use of a water-insulated transmission line inside an LTD module has several advantages over the use of a vacuum MITL. Water insulation eliminates the constraint that magnetic insulation be maintained everywhere in the MITL, at all times. A water line of a given length also allows a much wider range of pulse shapes, since for time scales of interest the dielectric constant of water is 80. Hence, for a given geometrical cavity length, the electrical length τ_c is a factor of 6 to 9 times greater for a water line than it is for a MITL, and the constraint given by Eq. (13) is that much less restrictive. In addition, a water line does not launch electron-flow current, which represents an energy loss, and which can damage hardware when the flow electrons are eventually lost downstream to an anode.

For pulse shape A, the peak voltage at the output of each of the 60 cavities is 106 kV. Assuming the anode-cathode

TABLE I. The highest peak voltage at the output of a cavity, highest peak electric field E_p, and associated effective pulse width τ_{eff} for each of current-pulse shapes A–F. The last column lists values of the expression $E_p\tau_{\text{eff}}^{0.33}$ assuming E_p is given in MV/cm and τ_{eff} in μs [54,55]. All the values of $E_p\tau_{\text{eff}}^{0.33}$ are significantly below the design criterion of 0.108 proposed in Refs. [54,55].

Current-pulse shape	Highest peak voltage at a cavity output (MV)	Highest peak electric field E_p (MV/cm)	Associated effective pulse width τ_{eff} (μs)	$E_p\tau_{\text{eff}}^{0.33}$
A	0.106	0.053	0.143	0.028
B	0.179	0.090	0.190	0.052
C	0.188	0.094	0.248	0.059
D	0.188	0.094	0.158	0.051
E	0.106	0.053	0.143	0.028
F	0.821	0.411	0.0083	0.084

(AK) gap at the cavity output is 2 cm, the peak electric field E_p is 53 kV/cm. The effective width of the pulse τ_{eff} (the full width at 63% of peak) is 143 ns. For shapes B–F, the peak voltage is different at each cavity; Table I gives for each shape the highest peak value and associated effective pulse width. Table I also lists an estimate of the peak value of the expression $E_p\tau_{\text{eff}}^{0.33}$ [54,55]. Since the gap at the cavity output would be water insulated, Table I and Refs. [54,55] suggest that the AK gaps at the outputs would not suffer dielectric failure, since each value of $E_p\tau_{\text{eff}}^{0.33}$ is less than 0.108.

Each of the five shapes plotted by Fig. 4 is a linear combination of 60 time-shifted pulses, each of which is produced by one of the module's 60 cavities. The pulses produced by six of the cavities are plotted by Fig. 6. The timing shown for these pulses is that achieved for cavity-triggering sequence A. Each of the six plots assumes the cavity's initial charge voltage is 200 kV. Of course, the amplitude of the pulse produced by a cavity could be reduced by reducing that cavity's initial voltage.

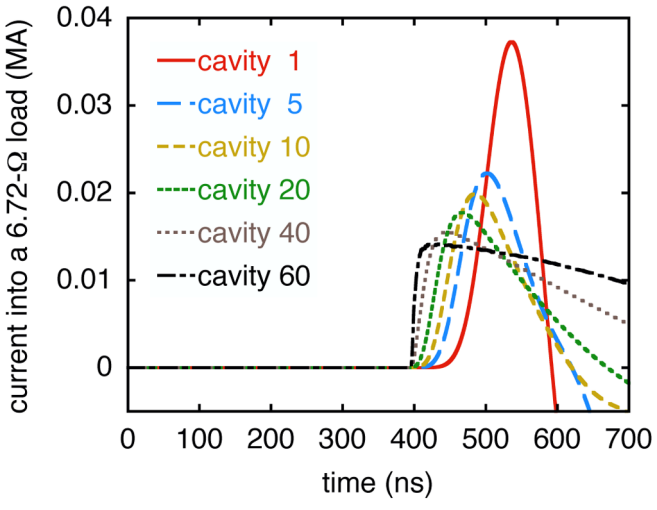

FIG. 6. (Color) The current pulses produced by six cavities of a 60-cavity LTD module. (The specific cavity timing indicated here is that which is produced by timing-sequence A.) Each of the five shapes plotted by Fig. 4 is a linear combination of 60 time-shifted pulses, each of which is produced by one of the module's 60 cavities.

TABLE II. The rise time for three different current-pulse shapes. For shape A, the switches of each cavity are closed at a time τ_c later than the closure of the switches in the cavity immediately *upstream*, where τ_c is the time it takes an electromagnetic pulse to propagate (down the internal transmission line) the length of a single cavity. For shape B, the switches in all the cavities are closed simultaneously. For shape C, the switches of each cavity are closed at a time τ_c later the cavity immediately *downstream*.

Current-pulse shape	10%–90% current-pulse rise time
A	53 ns
B	240 ns
C	297 ns

The 10%–90% rise times of current shapes A, B, and C (which are plotted by Fig. 4) are listed in Table II. When Eq. (13) is satisfied, the minimum rise time—and maximum peak electrical power—that can be achieved by the LTD module described above is that of current-shape A.

A general expression for the minimum rise time achievable by an LTD module under a certain set of conditions is developed in Appendix C. The maximum rise time, which is a function of n, τ_c, and the time histories of the pulses produced by each of the module's cavities, can be determined by performing circuit simulations.

III. PULSE SHAPING WHEN $|t_{j+1} - t_j| > \tau_c$

In this section we explore the effects of a deviation from the constraint imposed by Eq. (13). Figures 4 and 6 make clear that rise times shorter, and peak powers higher, than those of timing sequence A of Fig. 5 could, in principle, be achieved by bringing the peaks of the pulses of Fig. 6 into better temporal alignment. This could be achieved by triggering the switches of each cavity at a time later than τ_c seconds after the closure of the switches in the cavity immediately upstream. For such a timing sequence

$$t_{j+1} - t_j > \tau_c \tag{14}$$

for all the cavities of the module.

In Fig. 7 we plot a current pulse (labeled F) which is produced by one such timing sequence, for which

$$t_{j+1} - t_j = \tau_c + 1.4 \text{ ns} \tag{15}$$

for all the cavities. Figure 7 compares current shapes F and A. The rise time of shape F is 27 ns, a *factor of 2 less* than it is for A. The peak current of shape F is 9% higher; the peak electrical power delivered to the load is 20% higher.

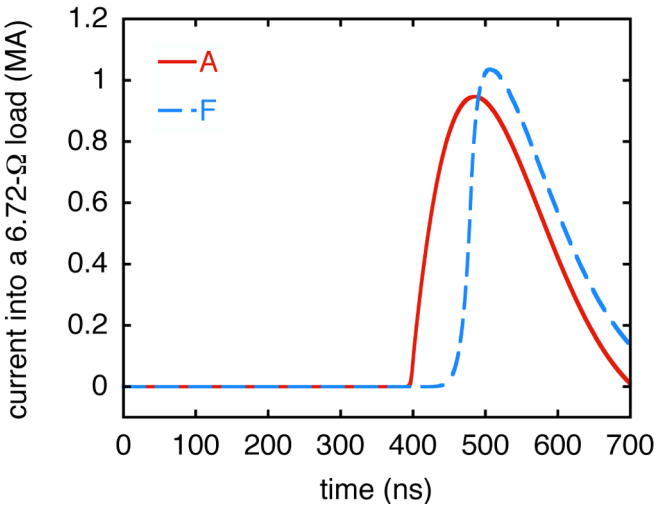

FIG. 7. (Color) Comparison of current-shape A with one that can be achieved when $t_{j+1} - t_j = \tau_c + 1.4$ ns, for all values of j between 1 and $n - 1$, where t_j is the time at which the switches of the jth cavity are triggered.

The peak power for shape A is a factor of n times the peak power that can be produced by an individual cavity, one that is not part of a module. It is interesting to note that the peak power for shape F is greater than that achieved by shape A: it is greater than the sum of the peak powers that can be produced by n individual cavities. Equation (15) assumes $t_{j+1} - t_j$ is the same for all the cavities; even higher peak powers could be achieved by a timing sequence for which $t_{j+1} - t_j$ is different for each of the cavities. Hence, it would appear that a substantial improvement in the performance of an LTD module is possible by using a timing sequence that satisfies Eq. (14).

However, as suggested by Fig. 8, the total energy in the primary power pulse is 8% less for F than it is for A.

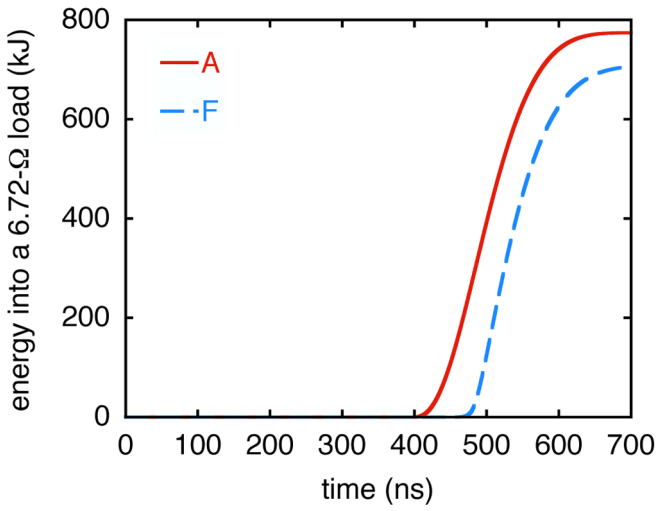

FIG. 8. (Color) The energy in the main power pulse for current shapes A and F.

Furthermore, the cavity timing sequence needed to produce shape F allows the voltage across a cavity to be altered by pulses produced by the other cavities of the module. For example, as suggested by Table I, shape F of Fig. 7 assumes that the 60th cavity could withstand an 821-kV pulse across its output before the switches are triggered. The switches presently envisioned for use in such cavities are designed to be charged to 200-kV dc, and may not withstand an 821-kV pulse before closing. The internal dielectric insulation of such cavities also may not withstand such a pulse.

Hence, additional technical advances may be necessary before one could realize the significant benefits of timing sequences for which the quantity $|t_{j+1} - t_j|$ exceeds τ_c. Nevertheless, present technology may allow slight deviations from Eq. (13) to achieve minor performance improvements.

IV. DISCUSSION

An even wider variety of pulse shapes than that suggested by Fig. 4 could be generated by the accelerator of Fig. 1. The accelerator has 210 LTD modules, each of which could be triggered at a different time. Viable timing sequences might be constrained by a transit-time isolation requirement similar to that given by Eq. (13); i.e., the switches of a module may need to be triggered before the voltage across a switch is affected by pulses produced by the other modules of the accelerator. Here again the use of water insulation (instead of vacuum) helps: The water-insulated radial-transmission-line impedance transformers of the accelerator [37,56] offer the advantage of longer transit times for given geometric distances. The 210 output pulses would be combined and symmetrized by the transformers [37,56]. Such an accelerator would have, in effect, $60 \times 210 = 12\,600$ switch points.

Moreover, each of the accelerator's LTD cavities would likely have many switches, on the order of 40, which need not be triggered simultaneously. If, for example, the 40 switches of a cavity were to be triggered in four groups of 10 [20], then such an accelerator would have 50 400 switch points. The timing sequence (of all the switches of the accelerator) that would be required to produce a given pulse shape could be determined using the genetic algorithm developed by Glover and co-workers [57,58]. The symmetrization of the 210 pulses by the impedance transformers could be evaluated with fully electromagnetic 3D simulations similar to the 2D calculations presented by Welch and colleagues in Ref. [56].

Throughout this article we make the simplifying assumptions that the impedance profile of a module's transmission line is that given by Eq. (1), and that each cavity has the same electrical length [Eq. (2)]. It would be of interest to explore the effects and possible advantages of other impedance and cavity-length profiles. It would also

be of interest to further evaluate cavity-timing sequences for which $|\tau_{j+1} - \tau_j|$ exceeds τ_c for one or more cavities.

ACKNOWLEDGMENTS

The authors would very much like to thank R. B. Spielman for upgrading the SCREAMER circuit code to make possible the calculations described herein, and G. L. Donovan, A. A. Kim, W. L. Langston, R. J. Leeper, L. X. Schneider, and J. W. Weed for critical discussions. The authors also gratefully acknowledge their many other colleagues at Sandia National Laboratories, EG&G, Institute of High Current Electronics, Ktech Corporation, L-3 Communications, and Voss Scientific for invaluable contributions. Sandia is a multiprogram laboratory operated by Sandia Corporation, a Lockheed Martin Company, for the United States Department of Energy's National Nuclear Security Administration under Contract No. DE-AC04-94AL85000.

APPENDIX A: LONG MITLS

Several previously described accelerator architectures assume the use of long MITLs (instead of long water-insulated transmission lines) to connect the accelerator's pulsed-power drivers to the central region of the accelerator. (In this context, a MITL is defined to be long when the rise time of the power pulse is less than the two-way transit time of the MITL.) The architecture illustrated by Fig. 1, which incorporates long water lines, represents a significant departure from such MITL-based designs. The use of long water lines follows naturally from the use of LTD modules that drive an internal water line, and eliminates electron-flow losses that are inherent in a long-MITL system.

A complete discussion of the advantages and disadvantages of the two types of architectures is outside the scope of the present article. However, we observe that a long-MITL architecture served as the basis for the design of the PBFA-I accelerator, which was built at Sandia National Laboratories [59]. When PBFA I was subsequently upgraded, its long MITLs were replaced with long water lines [60]. This was motivated in part by calculations presented in Ref. [59], which suggest that long water lines couple more efficiently than long MITLs to various loads, including z pinches. The PBFA-II, Z, and ZR accelerators, all built at Sandia after PBFA I, incorporated long water lines instead of long MITLs.

APPENDIX B: OPTIMUM OUTPUT IMPEDANCE OF THE INTERNAL TRANSMISSION LINE OF AN LTD MODULE

We estimate here the optimum output impedance $Z_{n,\mathrm{opt}}$ of the concentric transmission line that is located within, and is driven by, an LTD module that consists of n identical cavities connected in series. We define the optimum impedance to be that which maximizes the peak forward-going electrical power at the output of the module, under the constraints given by Eqs. (1), (2), and (13). When the module's transmission line is terminated in an impedance-matched load, the forward-going power is, of course, identical to the power delivered to the load.

Under the conditions given by Eqs. (1), (2), and (13), the peak power is maximized by the triggering sequence that satisfies Eq. (10). The discussion that follows extends that given in Appendix D of Ref. [37] (although we caution that the notation has been changed). We repeat here much of the discussion of Ref. [37] for completeness, and since the discussion is used for Appendix C.

We assume the LTD circuit model presented by Fig. 3(b). The model generalizes that proposed by Mazarakis and colleagues in Refs. [11,25] by including a parallel resistance to account for energy loss to the inductive magnetic cores of the LTD cavities. Considerably more accurate LTD circuit models are proposed by Kim and colleagues in Ref. [20] and Leckbee and co-workers in Refs. [24,28].

When Eqs. (1), (2), and (10) are satisfied throughout an LTD module, the circuit of Fig. 3(b) can be modeled as Fig. 3(c). Figure 3(c) represents an LTD module that consists of three identical LTD cavities connected in series. For a module consisting of n identical cavities in series,

$$R_{s,n} = nR_s, \tag{B1}$$

$$L_n = nL, \tag{B2}$$

$$C_n = C/n, \tag{B3}$$

$$R_{p,n} = nR_p, \tag{B4}$$

$$Z_n = nZ_1. \tag{B5}$$

The quantity $R_{s,n}$ is that part of the *series* resistance of an n-cavity LTD module due primarily to the switches and capacitors of the module. L_n and C_n are the series inductance and capacitance, respectively, of the module. $R_{p,n}$ is the effective *parallel* resistance of the module; this element is used to model the loss of energy to the module's magnetic cores. (We assume that nonlinearities due to the cores can be neglected.) The quantity Z_1 is the impedance of the transmission-line segment driven by the module's *first* cavity; Z_n is the impedance of the segment driven by the nth cavity, at the output of a module.

For an n-cavity version of Fig. 3(c), it is well known that the charge on the capacitance C_n (which we label as Q_n) and the current flowing through the circuit (I_n) are given as follows [37]:

$$Q_n(t) = Ae^{-\alpha t}\cos(\omega t + \beta), \tag{B6}$$

$$I_n(t) = -\omega A e^{-\alpha t}\sin(\omega t + \beta) - \alpha A e^{-\alpha t}\cos(\omega t + \beta)$$
$$= \frac{-V_n}{\omega L_n} e^{-\alpha t}\sin\omega t, \tag{B7}$$

where

$$A \equiv \frac{Q_n(t=0)}{\cos\beta} = \frac{C_n V_n}{\cos\beta}, \tag{B8}$$

$$V_n \equiv \frac{Q_n(t=0)}{C_n} = nV, \tag{B9}$$

$$\alpha \equiv \frac{R_n}{2L_n}, \tag{B10}$$

$$R_n \equiv R_{s,n} + \frac{Z_n R_{p,n}}{Z_n + R_{p,n}}, \tag{B11}$$

$$\omega^2 \equiv \frac{1}{L_n C_n} - \alpha^2, \tag{B12}$$

$$\beta \equiv \arctan\left(\frac{-\alpha}{\omega}\right). \tag{B13}$$

Equations (B6)–(B13) are valid whenever $\omega^2 > 0$. The quantity R_n is the total effective series resistance of the *RLC* circuit that represents an n-cavity LTD module [Fig. 3(c)]. The quantity V is the *initial* charge voltage across capacitance C. Equation (B9) assumes that the initial voltage is the same for each of the n cavities.

When its output transmission line is terminated in an impedance equal to Z_n (i.e., the impedance of the module's final transmission-line segment), the electrical power at the output of a module is given by

$$P_n = \left(\frac{R_{p,n}}{Z_n + R_{p,n}}\right)^2 I_n^2 Z_n. \tag{B14}$$

Equations (B1)–(B14) make clear that for the conditions considered in this Appendix,

$$P = \frac{P_n}{n} = \left(\frac{R_p}{Z_1 + R_p}\right)^2 I_n^2 Z_1, \tag{B15}$$

where P is the electrical power produced by a single cavity when it is not part of a module.

Appendix D of Ref. [37] finds that when $R_p, R_{p,n} \to \infty$; i.e., in the absence of magnetic-core losses, the optimum output impedance is given by the following expression:

$$Z_{n,\text{ideal}} = 1.10\sqrt{\frac{L_n}{C_n}} + 0.80 R_{s,n}. \tag{B16}$$

We estimate here the optimum output impedance when core losses are taken into account, and label this impedance as $Z_{n,\text{opt}}$. To estimate $Z_{n,\text{opt}}$ we use Eqs. (B1)–(B14), (B16), and dimensional analysis to observe that it may be possible

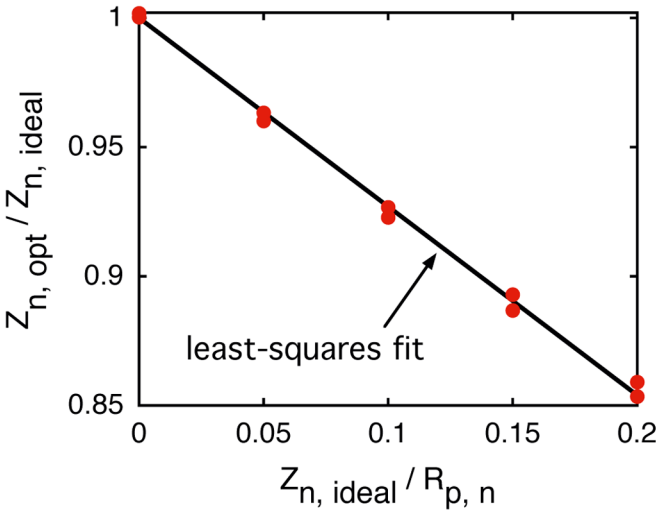

FIG. 9. (Color) The ratio $Z_{n,\text{opt}}/Z_{n,\text{ideal}}$ as a function of $Z_{n,\text{ideal}}/R_{p,n}$. The quantity $Z_{n,\text{opt}}$ is the LTD-module output impedance that maximizes the peak forward-going electrical power produced by a module, when Eqs. (1), (2), and (10) are satisfied; $Z_{n,\text{ideal}}$ is the optimum impedance in the absence of magnetic-core losses. $R_{p,n}$ is the effective parallel resistance of an LTD cavity module, and is included in the circuit model to account for energy loss to the module's magnetic cores.

to express the ratio $Z_{n,\text{opt}}/Z_{n,\text{ideal}}$ as a function only of the ratio $Z_{n,\text{ideal}}/R_{p,n}$:

$$\frac{Z_{n,\text{opt}}}{Z_{n,\text{ideal}}} = f\left(\frac{Z_{n,\text{ideal}}}{R_{p,n}}\right). \tag{B17}$$

Using Eqs. (B1)–(B14) we calculated $Z_{n,\text{opt}}/Z_{n,\text{ideal}}$ numerically at several values of $Z_{n,\text{ideal}}/R_{p,n}$. The results are plotted by Fig. 9. A least-squares analysis finds that to a reasonable approximation,

$$Z_{n,\text{opt}} = Z_{n,\text{ideal}}\left(1 - 0.73\frac{Z_{n,\text{ideal}}}{R_{p,n}}\right). \tag{B18}$$

Equations (B16) and (B18) are correct to $\sim 1\%$ whenever

$$\frac{R_{s,n}}{\sqrt{L_n/C_n}} < 0.5, \tag{B19}$$

$$\frac{Z_{n,\text{ideal}}}{R_{p,n}} \leq 0.2, \tag{B20}$$

and the LTD module can be modeled as suggested by Eqs. (B1)–(B14) and Fig. 3(c).

APPENDIX C: MINIMUM RISE TIME OF AN LTD MODULE

In this Appendix we estimate the minimum 10%–90% rise time $\tau_{r,\text{min}}$ of the forward-going current pulse at the output of an LTD module that consists of n-identical cavities connected in series. When the module is termi-

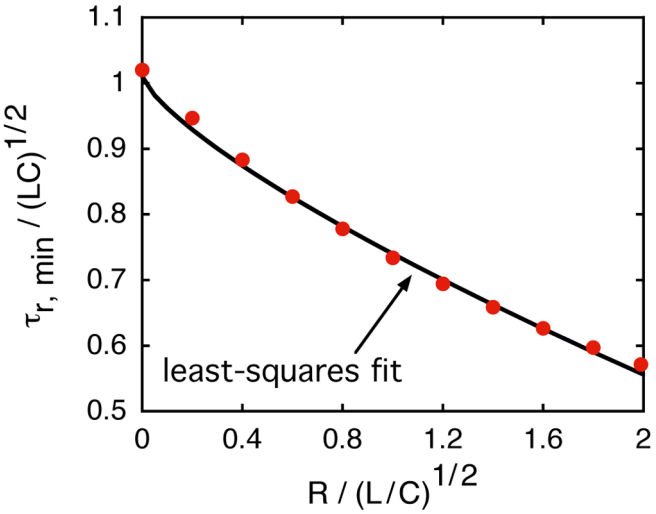

FIG. 10. (Color) The ratio $\tau_{r,\min}/\sqrt{LC}$ as a function of $R/\sqrt{L/C}$. The quantity $\tau_{r,\min}$ is the minimum current-pulse rise time that can be achieved by an impedance-matched LTD module when Eqs. (1), (2), and (10) are satisfied. L and C are the inductance and capacitance, respectively, of a single LTD cavity. R, which is defined by Eq. (C2), is the total effective series resistance of the RLC circuit that represents a single cavity.

nated in an impedance equal to Z_n, i.e., the impedance of the module's final transmission-line segment, the forward-going current is, of course, identical to the current delivered to the load. We define the minimum rise time to be that which is achieved when the peak forward-going power is maximized as discussed in Appendix B; hence, the minimum rise time we estimate below is that obtained under the constraints given by Eq. (1), (2), and (10).

We use Eqs. (B1)–(B13) and dimensional analysis to observe that it may be possible to express the ratio $\tau_{r,\min}/\sqrt{L_nC_n}$ as a function of only the ratio $\sqrt{L_nC_n}/(L_n/R_n)$, which can be expressed as $R_n/\sqrt{L_n/C_n}$:

$$\frac{\tau_{r,\min}}{\sqrt{L_nC_n}} = f\left(\frac{R_n}{\sqrt{L_n/C_n}}\right). \tag{C1}$$

It is clear Eq. (C1) is independent of n; we can make this explicit by defining

$$R \equiv R_s + \frac{Z_1R_p}{Z_1 + R_p} = \frac{R_n}{n} \tag{C2}$$

and expressing Eq. (C1) as

$$\frac{\tau_{r,\min}}{\sqrt{LC}} = f\left(\frac{R}{\sqrt{L/C}}\right). \tag{C3}$$

The quantity R is the total effective series resistance of the RLC circuit that represents a single LTD cavity when it is not part of a module.

Using Eqs. (B1)–(B13) we calculated $\tau_{r,\min}/\sqrt{LC}$ numerically at several values of $R/\sqrt{L/C}$. The results are plotted by Fig. 10. A least-squares analysis finds that to a reasonable approximation,

$$\tau_{r,\min} = \sqrt{LC}\left[1.01 - 0.27\left(\frac{R}{\sqrt{L/C}}\right)^{3/4}\right]. \tag{C4}$$

Equation (C4) is correct to within 3% whenever

$$\omega^2 > 0 \tag{C5}$$

and the LTD module can be modeled as suggested by Eqs. (B1)–(B13) and Fig. 3(c).

[1] B. M. Kovalchuk, V. A. Vizir, A. A. Kim, E. V. Kumpjak, S. V. Loginov, A. N. Bastrikov, V. V. Chervjakov, N. V. Tsou, Ph. Monjaux, and D. Huet, Russ. Phys. J. **40**, 1142 (1997).

[2] B. M. Kovalchuk, in *Proceedings of the 11th IEEE International Pulsed Power Conference*, edited by G. Cooperstein and I. Vitkovitsky (IEEE, Piscataway, NJ, 1997), p. 59.

[3] A. N. Bastrikov, A. A. Kim, B. M. Kovalchuk, E. V. Kumpjak, S. V. Loginov, V. I. Manylov, V. A. Visir, V. P. Yakovlev, B. Etlicher, A. Chiuvatin, L. Frescaline, J. F. Leon, P. Monjaux, F. Kovacs, D. Huet, and F. Bayol, in Proceedings of the 11th IEEE International Pulsed Power Conference (Ref. [2]), p. 489.

[4] A. A. Kim, B. M. Kovalchuk, V. V. Kremnev, E. V. Kumpjak, A. A. Novikov, B. Etlicher, L. Frescaline, J. F. Leon, B. Roques, F. Lassalle, R. Lample, G. Avrillaud, and F. Kovacs, in Proceedings of the 11th IEEE International Pulsed Power Conference (Ref. [2]), p. 862.

[5] B. M. Kovalchuk and A. A. Kim (unpublished).

[6] M. G. Mazarakis and R. B. Spielman, in *Proceedings of the 12th IEEE International Pulsed Power Conference*, edited by C. Stallings and H. Kirbie (IEEE, Piscataway, NJ, 1999), p. 412.

[7] A. A. Kim, B. M. Kovalchuk, E. V. Kumpjak, and N. V. Zoi, in Proceedings of the 12th IEEE International Pulsed Power Conference (Ref. [6]), p. 955.

[8] M. G. Mazarakis and R. B. Spielman, in *Proceedings of the 20th International Linac Conference* (Stanford Linear Accelerator Center Report SLAC-R-561), edited by A. W. Chao (Stanford Linear Accelerator Center, Stanford, CA, 2000), p. 497.

[9] A. A. Kim and B. M. Kovaltchuk, in *Proceedings of the 12th Symposium on High Current Electronics*, edited by G. Mesyats, B. Kovalchuk, and G. Remnev (Institute of High Current Electronics, Tomsk, Russia, 2000), p. 263.

[10] P. Corcoran, I. Smith, P. Spence, A. R. Miller, E. Waisman, C. Gilbert, W. Rix, P. Sincerny, L. Schlitt, and D. Bell, in *Proceedings of the 13th IEEE International Pulsed Power Conference*, edited by R. Reinovsky and M. Newton (IEEE, Piscataway, NJ, 2001), p. 577.

[11] M. G. Mazarakis, R. B. Spielman, K. W. Struve, and F. W. Long, in Proceedings of the 13th IEEE International Pulsed Power Conference (Ref. [10]), p. 587.

[12] B. M. Kovalchuk, A. A. Kim, E. V. Kumpjak, N. V. Zoi, and V. B. Zorin, in Proceedings of the 13th IEEE

International Pulsed Power Conference (Ref. [10]), p. 1488.

[13] A. A. Kim, B. M. Kovalchuk, A. N. Bastrikov, V. G. Durakov, S. N. Volkov, and V. A. Sinebryukhov, in Proceedings of the 13th IEEE International Pulsed Power Conference (Ref. [10]), p. 1491.

[14] I. Smith, P. Corcoran, A. R. Miller, V. Carboni, P. Sincerny, P. Spence, C. Gilbert, W. Rix, E. Waisman, L. Schlitt, and D. Bell, IEEE Trans. Plasma Sci. **30**, 1746 (2002).

[15] A. A. Kim, A. N. Bastrikov, S. N. Volkov, V. G. Durakov, B. M. Kovalchuk, and V. A. Sinebryukhov, in *Proceedings of the 14th International Conference on High-Power Particle Beams (Beams 2002)*, edited by T. A. Mehlhorn and M. A. Sweeney, AIP Conf. Proc. No. 650 (AIP, Melville, NY, 2002), p. 81.

[16] A. N. Bastrikov, V. A. Vizir, S. N. Volkov, V. G. Durakov, A. M. Efremov, V. B. Zorin, A. A. Kim, B. M. Kovalchuk, E. V. Kumpjak, S. V. Loginov, V. A. Sinebryuhov, N. V. Tsou, V. V. Cervjakov, V. P. Yakovlev, and G. A. Mesyats, Laser Part. Beams **21**, 295 (2003).

[17] D. V. Rose, D. R. Welch, B. V. Oliver, J. E. Maenchen, D. C. Rovang, D. L. Johnson, A. A. Kim, and B. M. Kovalchuk, in *Proceedings of the 14th IEEE International Pulsed Power Conference*, edited by M. Giesselmann and A. Neuber (IEEE, Piscataway, NJ, 2003), p. 845.

[18] A. A. Kim, A. N. Bastrikov, S. N. Volkov, V. G. Durakov, B. M. Kovalchuk, and V. A. Sinebryukhov, in Proceedings of the 14th IEEE International Pulsed Power Conference (Ref. [17]), p. 853.

[19] B. M. Kovalchuk, A. A. Kim, E. V. Kumpjak, and N. V. Tsou, in Proceedings of the 14th IEEE International Pulsed Power Conference (Ref. [17]), p. 1455.

[20] A. A. Kim, A. N. Bastrikov, S. N. Volkov, V. G. Durakov, B. N. Kovalchuk, and V. A. Synebrukhov, in *Proceedings of the 13th International Symposium on High Current Electronics*, edited by B. Kovalchuk and G. Remnev (Institute of High Current Electronics, Tomsk, Russia, 2004), p. 141.

[21] V. A. Vizir, A. D. Maksimenko, V. I. Manylov, and G. V. Smorudov, in Proceedings of the 13th International Symposium on High Current Electronics (Ref. [20]), p. 198.

[22] J. Leckbee, J. Maenchen, S. Portillo, S. Cordova, I. Molina, D. L. Johnson, A. A. Kim, R. Chavez, and D. Ziska, in *Proceedings of the 15th IEEE International Pulsed Power Conference*, edited by J. Maenchen and E. Schamiloglu (IEEE, Piscataway, NJ, 2005), p. 132.

[23] S. T. Rogowski, W. E. Fowler, M. G. Mazarakis, C. L. Olson, D. H. McDaniel, K. W. Struve, and R. A. Sharpe, in Proceedings of the 15th IEEE International Pulsed Power Conference (Ref. [22]), p. 155.

[24] J. Leckbee, J. Maenchen, S. Portillo, S. Corodova, I. Molina, D. L. Johnson, D. V. Rose, A. A. Kim, R. Chavez, and D. Ziska, in Proceedings of the 15th IEEE International Pulsed Power Conference (Ref. [22]), p. 386.

[25] M. G. Mazarakis, W. E. Fowler, F. W. Long, D. H. McDaniel, C. L. Olson, S. T. Rogowski, R. A. Sharpe, K. W. Struve, and A. A. Kim, in Proceedings of the 15th IEEE International Pulsed Power Conference (Ref. [22]), p. 390.

[26] C. L. Olson, in *Landholt-Boernstein Handbook on Energy Technologies*, edited by W. Martienssen, Fusion Technologies, edited by K. Heinloth (Springer-Verlag, Berlin-Heidelberg, 2005), Vol. VIII/3.

[27] D. V. Rose, D. R. Welch, B. V. Oliver, J. J. Leckbee, J. E. Maenchen, D. L. Johnson, A. A. Kim, B. M. Kovalchuk, and V. A. Sinebryukhov, IEEE Trans. Plasma Sci. **34**, 1879 (2006).

[28] J. J. Leckbee, J. E. Maenchen, D. L. Johnson, S. Portillo, D. M. Van De Valde, D. V. Rose, and B. V. Oliver, IEEE Trans. Plasma Sci. **34**, 1888 (2006).

[29] M. G. Mazarakis, W. E. Fowler, D. H. McDaniel, A. A. Kim, C. L. Olson, S. T. Rogowski, R. A. Sharpe, and K. W. Struve, in *Proceedings of the 14th Symposium on High Current Electronics*, edited by B. Kovalchuk and G. Remnev (Institute of High Current Electronics, Tomsk, Russia, 2006), p. 226.

[30] A. A. Kim, V. G. Durakov, S. N. Volkov, A. N. Bastrikov, B. M. Kovalchuk, V. A. Sinebryukhov, S. V. Frolov, V. M. Alexeenko, L. Véron, M. Toury, C. Vermare, R. Nicloas, F. Bayol, and C. Drouilly, in Proceedings of the 14th Symposium on High Current Electronics (Ref. [29]), p. 297.

[31] M. G. Mazarakis, W. E. Fowler, D. H. McDaniel, A. A. Kim, C. L. Olson, S. T. Rogowski, R. A. Sharpe, and K. W. Struve, in *Proceedings of the 2006 International Conference on Megagauss Magnetic Field Generation and Related Topics*, edited by G. F. Kiuttu, R. E. Reinovsky, and P. J. Turchi (IEEE, Piscataway, NJ, 2007), p. 523.

[32] M. G. Mazarakis and K. W. Struve, Sandia National Laboratories Report number SAND2006-5811, 2006.

[33] A. Kim, V. Sinebryukhov, B. Kovalchuk, A. Bastrikov, V. Durakov, S. Volkov, S. Frolov, V. Alexeenko, M. Mazarakis, D. McDaniel, C. Olson, K. Struve, and R. Gilgenbach, in *Proceedings of the 16th IEEE International Pulsed Power Conference*, edited by E. Schamiloglu and F. Peterkin (IEEE, Piscataway, NJ, 2007), p. 144.

[34] A. Kim, V. Sinebryukhov, B. Kovalchuk, A. Bastrikov, V. Durakov, S. Volkov, S. Frolov, V. Alexeenko, F. Bayol, F. Cubaynes, C. Drouilly, L. Véron, M. Toury, and C. Vermare, in Proceedings of the 16th IEEE International Pulsed Power Conference (Ref. [33]), p. 148.

[35] M. R. Gomez, R. M. Gilgenbach, Y. Y. Lau, W. Tang, J. C. Zier, M. G. Mazarakis, M. E. Cuneo, T. A. Mehlhorn, and W. A. Stygar, in Proceedings of the 16th IEEE International Pulsed Power Conference (Ref. [33]), p. 152.

[36] M. G. Mazarakis, W. E. Fowler, D. H. McDaniel, C. L. Olson, S. T. Rogowski, R. A. Sharpe, K. W. Struve, W. A. Stygar, A. A. Kim, V. A. Sinebryukhov, R. M. Gilgenbach, and M. R. Gomez, in Proceedings of the 16th IEEE International Pulsed Power Conference (Ref. [33]), p. 222.

[37] W. A. Stygar, M. E. Cuneo, D. I. Headley, H. C. Ives, R. J. Leeper, M. G. Mazarakis, C. L. Olson, J. L. Porter, T. C. Wagoner, and J. R. Woodworth, Phys. Rev. ST Accel. Beams **10**, 030401 (2007).

[38] I. D. Smith, Phys. Rev. ST Accel. Beams **7**, 064801 (2004).

[39] D. B. Reisman, A. Toor, R. C. Cauble, C. A. Hall, J. R. Asay, M. D. Knudson, and M. D. Furnish, J. Appl. Phys. **89**, 1625 (2001).

[40] C. A. Hall, J. R. Asay, M. D. Knudson, W. A. Stygar, R. B. Spielman, T. D. Pointon, D. B. Reisman, A. Toor, and R. C. Cauble, Rev. Sci. Instrum. **72**, 3587 (2001).
[41] M. D. Knudson, D. L. Hanson, J. E. Bailey, C. A. Hall, J. R. Asay, and W. W. Anderson, Phys. Rev. Lett. **87**, 225501 (2001).
[42] J.-P. Davis, C. Deeney, M. D. Knudson, R. W. Lemke, T. D. Pointon, and D. E. Bliss, Phys. Plasmas **12**, 056310 (2005).
[43] R. W. Lemke, M. D. Knudson, D. E. Bliss, K. Cochrane, J.-P. Davis, A. A. Giunta, H. C. Harjes, and S. A. Slutz, J. Appl. Phys. **98**, 073530 (2005).
[44] J. P. Chittenden, S. V. Lebedev, J. Ruiz-Camacho, F. N. Beg, S. N. Bland, C. A. Jennings, A. R. Bell, M. G. Haines, S. A. Pikuz, T. A. Shelkovenko, and D. A. Hammer, Phys. Rev. E **61**, 4370 (2000).
[45] J. P. Chittenden, S. V. Lebedev, S. N. Bland, A. Ciardi, and M. G. Haines, Phys. Plasmas **8**, 675 (2001).
[46] F. N. Beg, S. V. Lebedev, S. N. Bland, J. P. Chittenden, A. E. Dangor, and M. G. Haines, Phys. Plasmas **9**, 375 (2002).
[47] S. V. Lebedev, F. N. Beg, S. N. Bland, J. P. Chittenden, A. E. Dangor, and M. G. Haines, Phys. Plasmas **9**, 2293 (2002).
[48] M. G. Mazarakis, J. W. Poukey, D. C. Rovang, J. E. Maenchen, S. R. Cordova, P. R. Menge, R. Pepping, L. Bennett, K. Mikkelson, D. L. Smith, J. Halbleib, W. A. Stygar, and D. R. Welch, Appl. Phys. Lett. **70**, 832 (1997).
[49] K. Hahn, B. V. Oliver, M. D. Johnston, S. Portillo, J. Leckbee, D. C. Rovang, I. Molina, S. Cordova, G. Cooper, J. McLean, D. R. Welch, N. Bruner, and D. V. Rose, in Proceedings of the 16th IEEE International Pulsed Power Conference (Ref. [33]), p. 794.
[50] M. L. Kiefer and M. M. Widner, in *Proceedings of the 5th IEEE International Pulsed Power Conference*, edited by M. F. Rose and P. J. Turchi (IEEE, Piscataway, NJ, 1985), p. 685.
[51] M. L. Kiefer, K. L. Shaw, K. W. Struve, M. M. Widner, and R. B. Spielman, SCREAMER, a pulsed power design tool, user's guide for version 3.2.4.2 (2008).
[52] R. B. Spielman (unpublished).
[53] M. E. Savage (unpublished).
[54] W. A. Stygar, T. C. Wagoner, H. C. Ives, Z. R. Wallace, V. Anaya, J. P. Corley, M. E. Cuneo, H. C. Harjes, J. A. Lott, G. R. Mowrer, E. A. Puetz, T. A. Thompson, S. E. Tripp, J. P. VanDevender, and J. R. Woodworth, Phys. Rev. ST Accel. Beams **9**, 070401 (2006).
[55] W. A. Stygar, M. E. Savage, T. C. Wagoner, L. F. Bennett, J. P. Corley, G. L. Donovan, D. L. Fehl, H. C. Ives, K. R. LeChien, G. T. Leifeste, F. W. Long, R. G. McKee, J. A. Mills, J. K. Moore, J. J. Ramirez, B. S. Stoltzfus, K. W. Struve, and J. R. Woodworth, Phys. Rev. ST Accel. Beams **12**, 010402 (2009).
[56] D. R. Welch, T. C. Genoni, D. V. Rose, N. L. Bruner, and W. A. Stygar, Phys. Rev. ST Accel. Beams **11**, 030401 (2008).
[57] S. F. Glover, K. W. Reed, F. E. White, and M. L. Harden, in Proceedings of the 16th IEEE International Pulsed Power Conference (Ref. [33]), p. 226.
[58] S. F. Glover, K. W. Reed, F. E. White, and M. L. Harden, IEEE Trans. Plasma Sci. **37**, 339 (2009).
[59] J. P. VanDevender, G. W. Barr, J. T. Crow, S. A. Goldstein, D. H. McDaniel, K. F. McDonald, T. H. Martin, W. B. S. Moore, E. L. Neau, G. D. Peterson, J. F. Seamen, D. B. Seidel, R. B. Spielman, B. N. Turman, G. Yonas, and I. D. Smith, in *Proceedings of the 4th International Topical Conference on High-Power Electron and Ion Beam Research and Technology (Beams '81)*, edited by H. J. Doucet and J. M. Buzzi (Ecole Polytechnique, Palaiseau, France, 1981), p. 725.
[60] D. D. Bloomquist, R. W. Stinnett, D. H. McDaniel, J. R. Lee, A. W. Sharpe, J. A. Halbleib, L. G. Schlitt, P. W. Spence, and P. Corcoran, in *Proceedings of the 6th IEEE International Pulsed Power Conference*, edited by P. J. Turchi and B. H. Bernstein (IEEE, Piscataway, NJ, 1987), p. 310.